Contact Topology and the Classification of Disclination Lines in Cholesteric Liquid Crystals

Joseph Pollard[1,*] and Gareth P. Alexander[2,†]
[1]Department of Physics, Durham University, Durham, DH1 3LE, United Kingdom
[2]Department of Physics and Centre for Complexity Science, University of Warwick, Coventry, CV4 7AL, United Kingdom

(Received 2 December 2022; accepted 16 May 2023; published 1 June 2023)

We give a complete topological classification of defect lines in cholesteric liquid crystals using methods from contact topology. By focusing on the role played by the chirality of the material, we demonstrate a fundamental distinction between "tight" and "overtwisted" disclination lines not detected by standard homotopy theory arguments. The classification of overtwisted lines is the same as nematics, however, we show that tight disclinations possess a topological layer number that is conserved as long as the twist is nonvanishing. Finally, we observe that chirality frustrates the escape of removable defect lines, and explain how this frustration underlies the formation of several structures observed in experiments.

DOI: 10.1103/PhysRevLett.130.228102

Many liquid crystal textures are distinguished by topological invariants derived from homotopy theory [1–3]. The classification of defects and solitons, both two- and three-dimensional, using homotopy groups is central to the modern understanding of liquid crystals and their properties [4–7]. However, despite the successes of homotopy theory methods, it has long been recognized that they are insufficient to fully describe materials with a spatially modulated ground state, such as smectics and cholesterics [8–10].

Cholesterics are characterized by the property that the director field $\mathbf{n}$ has everywhere a uniform sense of twist, $\mathbf{n} \cdot \nabla \times \mathbf{n} < 0$ for a right-handed material. This constraint on the twist is central to the rich morphology of structures displayed by cholesteric materials [7,11–18], but it is not accounted for in homotopy theory arguments, and standard topological invariants often fail to distinguish between qualitatively distinct cholesteric configurations [19]. The nonvanishing of the twist implies that the director defines a "contact structure" [20]. Techniques and insights from the field of contact topology go beyond the existing homotopy theory and are becoming increasingly important in the study of cholesteric materials following their introduction by Machon [19]. They have been used to demonstrate the preservation of the layer structure in a cholesteric [19]; to describe chiral point defects and elucidate the role of boundary conditions in the stability of complex defect structures in spherical droplets [21]; to explain the stability of Skyrmions in liquid crystals and chiral magnets [22]; to analyze defect structures in cylindrical capillaries [23]; and to shed light on the transition pathways between different cholesteric textures [24]. The mathematical formalism is developed only for nonsingular textures, i.e., without defects. The application of contact methods to defects was first made in [21] for point defects. Here, we extend this to disclination lines, both refining the existing homotopy theory and extending the mathematical framework.

A classification of defect lines in cholesterics was first given by Kleman and Friedel [25] who identified three classes, the χ lines (defects in the director), λ lines (defects in the pitch axis), and τ lines (defects in the director and pitch), and subsequently placed within the homotopy theory of defects [26,27]. This approach puts the pitch axis on equal footing with the director, even though it is only the latter that appears in the free energy. More subtly, it does not build in a consistent handedness (sense of twist). More recent geometric approaches take the pitch axis to be derived from the director gradients [28–30] and constrain the handedness by adopting methods of contact geometry [19,21–24] and it is this approach that we employ here. We give a complete classification of the local structure of disclination lines in cholesterics. This splits into two cases, corresponding to tight and overtwisted contact structures. For overtwisted disclinations, the classification is the same as in nematics. However, tight disclinations possess a topological layer number that is conserved as long as the twist does not vanish, resulting in a much finer topological classification.

We discuss how the classification applies to experimental situations including wedge geometries, colloidal inclusions, droplets, and blue phases. The methods we make use of have wider applicability in the analysis of chiral textures, which we illustrate for changes in layer structure,

Published by the American Physical Society under the terms of the Creative Commons Attribution 4.0 International license. Further distribution of this work must maintain attribution to the author(s) and the published article's title, journal citation, and DOI.

skyrmions, and hopfions. The method of analysis can also be applied naturally to existing three-dimensional imaging techniques such as fluorescent confocal polarizing microscopy [31,32]. We first describe explicit representatives of each of the homotopy classes and how they relate to the Kleman-Friedel nomenclature, deferring a sketch proof using contact topology to the end.

Our classification can be contrasted with the nematic case, where there is no constraint on the handedness. In nematics there are four homotopy classes for the local structure on the tubular neighborhood of a defect loop [4,13,33]. Representatives for each class are

$$\mathbf{n} = \cos\left(\frac{1}{2}\theta + \frac{\nu}{2}\phi\right)\mathbf{e}_x + \sin\left(\frac{1}{2}\theta + \frac{\nu}{2}\phi\right)\mathbf{e}_y, \qquad (1)$$

where θ, ϕ are the meridional and longitudinal angles, and $\nu \in \mathbb{Z}_4$ is the Jänich index. In the case $\nu = 0$ this extends to the global director field for a charge zero defect loop first given by Friedel and de Gennes [34,35]. It is a feature of these that the form of the director field (1) is independent of the geometry of the defect loop, whose shape and orientation can be arbitrary relative to the xy plane in which the director rotates. Such defect loops are not chiral and $\mathbf{n} \cdot \nabla \times \mathbf{n}$ takes both signs in the neighborhood of the defect [35]. In contrast, chiral defect loops have a director structure that is more closely connected to the geometry of the defect line in order to maintain a consistent handedness.

A tubular neighborhood of the defect loop is a solid torus [see the schematic in Fig. 1(a)] and so it suffices to classify textures on $D^2 \times S^1$, with a singular line along the central axis $0 \times S^1$, up to homotopies that fix the singular line and such that the twist $\mathbf{n} \cdot \nabla \times \mathbf{n}$ never vanishes. This classification splits into two cases: "tight" and "overtwisted," reflecting a fundamental dichotomy in contact topology. Informally a director is overtwisted if it contains a Skyrmion with a full π twist [19]. Contact topology tells us that tight director fields cannot be transformed into overtwisted ones without either the introduction of additional defects or the twist density $\mathbf{n} \cdot \nabla \times \mathbf{n}$ vanishing [19]. Further, Eliashberg's theorem [36] implies that overtwisted disclination lines have the same classification as nematic defects and do not possess any additional invariants as a result of their chirality. Thus the classification of overtwisted disclination loops is the same as that for nematics and given by a Jänich index $\nu \in \mathbb{Z}_4$. It remains to classify the tight disclinations. These are given by distinct classes of "dividing curves" on the boundary of the tubular neighborhood of the defect to be described presently; see also Fig. 1.

We now give representatives of each of the tight homotopy classes. We use polar coordinates (r, θ) for points of D^2 and an angular coordinate ϕ along S^1. We take the solid angle framing [37] to define the zero of the local azimuthal angle θ and let $\{\mathbf{e}_1, \mathbf{e}_2, \mathbf{e}_3\}$ be an adapted orthonormal frame with $\mathbf{e}_3$ tangent to the defect line and $\mathbf{e}_1$ the normal vector in the direction $\theta = 0$. The representatives can be distinguished according to the direction of the pitch axis, either parallel or perpendicular to the defect line, the former being the case for χ lines and the latter for τ lines. When the pitch is parallel to the defect axis we have a two-parameter family (of χ lines)

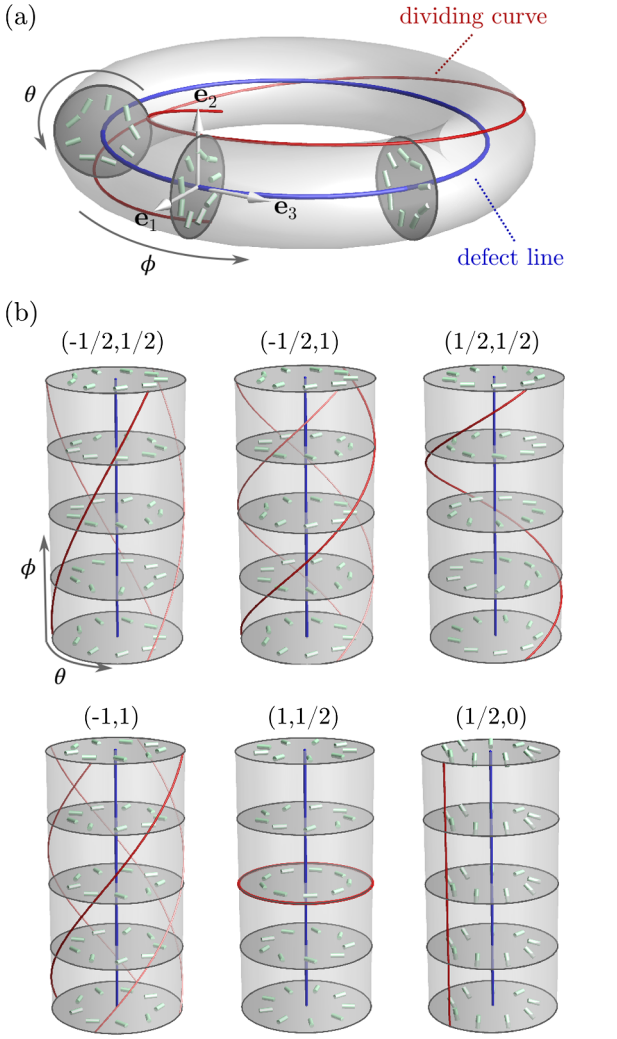

FIG. 1. (a) Schematic of the tubular neighborhood of a defect line (blue) with the director (green cylinders) shown on some cross-sections and part of the dividing curve (red). The frame $\{\mathbf{e}_1, \mathbf{e}_2, \mathbf{e}_3\}$ is shown on one cross section. The schematic corresponds to the representative texture $\mathbf{n}_{-1/2,1}$. (b) Examples from the family of tight cholesteric disclinations (2) for a selection of values of (k, q), shown in abstracted, standardized form. The examples include the "exceptional" cases $k = 1$ and $q = 0$ (3), where the dividing curve has either zero or infinite slope. Where the dividing curve has more than one component, one of them has been displayed in darker shade to aid visualization. The dividing curve facilitates the computation of invariants associated with the tight disclination in a manner described in the text.

$$\mathbf{n}^{\chi}_{k,q} = \cos(k\theta + q\phi)\mathbf{e}_1 + \sin(k\theta + q\phi)\mathbf{e}_2, \tag{2}$$

where k is an arbitrary half-integer, the winding number of the director in the disk D^2, and $q > 0$ is a positive half-integer giving the number of twists of the director along the S^1. When the pitch is perpendicular to the defect line, representatives can be given as the one-parameter family

$$\mathbf{n}^{\mathrm{az}}_{k} = \cos(k\theta)\mathbf{e}_3 + \sin(k\theta)\mathbf{e}_r, \tag{3}$$

where the pitch axis is oriented azimuthally. Here, $k > 0$ is a positive half-integer and $\mathbf{e}_r$ is the unit radial vector normal to the defect line. The more familiar form of τ lines is given by instead taking the pitch axis along a vector field $\mathbf{m}_k$ in the $\{\mathbf{e}_1, \mathbf{e}_2\}$ plane with winding number k (any half-integer) and setting

$$\mathbf{n}^{\tau}_{k} = \sin\psi\mathbf{e}_3 + \cos\psi\mathbf{m}_k \times \mathbf{e}_3, \tag{4}$$

where ψ is a helical phase increasing along the pitch axis. Several examples are shown in Fig. 1(b). Every tight disclination line is a chiral material that has a neighborhood homotopic to exactly one of these models.

Examples arise naturally in a Grandjean-Cano wedge geometry [38–40], where the cholesteric ground state is disrupted by the introduction of defects. These may be a $\lambda^{-1/2}\lambda^{+1/2}$ pair, but can also be pairs of defects consisting of a $\lambda^{\pm 1/2}$ line and a disclination line of type $\mathbf{n}^{\tau}_{\mp 1/2}$. Patterned substrates can be used to stabilize webs of disclinations of type $\mathbf{n}^{\tau}_{+1/2}$ [41], and disclinations of type $\mathbf{n}^{\tau}_{-1/2}$ occur around colloidal inclusions, in the well-known saturn ring texture [12,13]. Here, the homeotropic anchoring on the boundary of colloid implies the existence of a region of revered handedness close to the colloid [21], which region may either be nonsingular, or coupled to the defect itself. Disclinations with the same structure as the type $\mathbf{n}^{\chi}_{-1/2,1}$ disclination have been generated around colloidal inclusions [12,13], and $\mathbf{n}^{\chi}_{-1/2,1}$ disclinations also occur in all of the known blue phases [11].

We now give a proof of the classification, making use of three concepts from contact topology: convex surface theory, the Thurston-Bennequin invariant, and the tight-overtwisted dichotomy. We describe these concepts briefly; a more complete account can be found in [19,20]. Convex surface theory is a general tool for studying topological and geometrical properties of ordered media [20,42,43]. Consider an embedded surface S, either closed or with boundary orthogonal to the director, that does not intersect any defects. The director will be tangent to S along a collection of disjoint curves Γ that divide S into regions where the director points out of the surface, a set S^+, and regions where it points into the surface, S^-. This situation is generic: S is called a convex surface and Γ a dividing curve. A convex surface cutting across a cholesteric texture containing several λ-lines is shown in Fig. 2(a). The director is shown in the left half of the panel, with colors indicating whether it points into (blue) or out of (orange) the surface; on the right half of the panel we show only the dividing curve (red).

The dividing curve allows us to compute local topological information. For instance, it determines the Skyrmion charge Q on S via the formula

$$2Q = \chi_E(S^+) - \chi_E(S^-), \tag{5}$$

where χ_E denotes the Euler characteristic. We remark that under the nematic symmetry $\mathbf{n} \to -\mathbf{n}$ the two sets $S^{\pm}$ are interchanged leading to a reversal in the sign of the

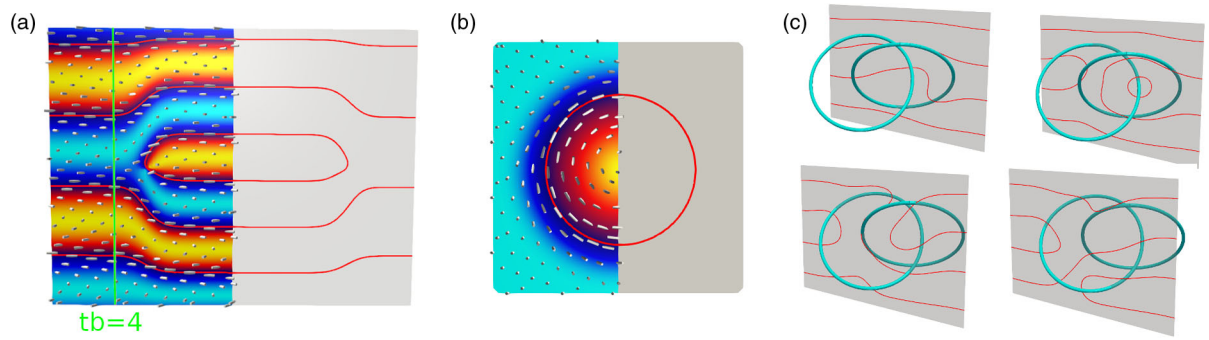

FIG. 2. Illustrations of convex surfaces, their dividing curves, and the computation of the Thurston-Bennequin (TB) number. (a) A convex torus (gray) cutting across a cholesteric texture exhibiting a change in the number of layers. The director, shown as white sticks, points out from the surface in orange regions and into the surface in blue regions. The topological content of this data is entirely captured by the dividing curve (red), the set of points where the director is tangent to the convex surface. The green line indicates an example calculation of a Thurston-Bennequin number. (b) On a convex surface cutting across a Skyrmion, the dividing curve is a closed contractible loops. By Giroux's criterion the contact structure is overtwisted. (c) Convex surface tomography of a Hopfion. As the convex surface is slid across the Hopfion, changes in the dividing curve track the changes in the layer structure. The presence of a closed component bounding a disk (top right) reveals the presence of a Skyrmion, with a local structure equivalent to that shown in panel (b) and shows that the Hopfion is overtwisted. The pale blue curves indicate the linked λ^{+1} lines of the Hopfion.

Skyrmion charge: this is well-known ambiguity in the sign of hedgehog (Skyrmion) charge in nematics [4,21].

We illustrate (5) for a single Skyrmion in Fig. 2(b). The region S^+ is a disk, with $\chi_E(S^+) = 1$. The remainder is a punctured plane, with $\chi_E(S^-) = -1$, so that (5) gives $Q = 1$. A similar calculation shows that the director in Fig. 2(a) also has $Q = 1$. In the case of a spherical surface the same formula (5) determines the point defect charge enclosed by S [44].

These properties of convex surfaces and dividing curves apply generally, including for achiral materials. However, in chiral materials we can also compute invariants connected to the nonzero twist. One is the Thurston-Bennequin invariant, which informally represents a count of the number of cholesteric layers [19]. Given a closed curve C that is everywhere orthogonal to the director, called a Legendrian curve, its Thurston-Bennequin number $\mathrm{tb}(C)$ is the number of right-handed π rotations of the director as one moves around C [45]. For such a curve on a surface which intersects the dividing curve transversely its Thurston-Bennequin number is the count of intersections between the curves

$$\mathrm{tb}(C) = |\Gamma \cap C|. \tag{6}$$

An example computation is shown in Fig. 2(a) for a standard cholesteric texture with λ lines and an extra layer. The minimum value of $\mathrm{tb}(C)$ over all curves in a given isotopy class, which we denote $\overline{\mathrm{tb}}$, is a topological invariant [19,20]. For the example shown, this is a count of the number of cholesteric layers.

More complex textures, such as the Hopfion shown in Fig. 2(c), can be visualized by studying the dividing curves on a series of slices through the material, a process called "tomography." Changes in the number of components of the dividing curve, and thus the minimal Thurston-Bennequin number attainable for a curve on each given slice, reveal fundamental changes in local topology.

For a disclination, the boundary of a tubular neighborhood serves as a convex surface S. Generically, the director will not be orthogonal to the disks D_ϕ of constant ϕ and hence we can take its projection into these disks. We refer to this projection as the profile of the line. On each D_ϕ the profile winds around the disclination with some half-integer winding number k_ϕ. As the dividing curve is identified with the points where the director is tangent to S, the number of intersections between Γ and the boundary of D_ϕ is $2|1 - k_\phi|$. The winding k_ϕ need not be constant and can vary with ϕ. We distinguish two cases: when k_ϕ is the same for all ϕ, and when it varies. In the latter case there are two ways in which the number of intersections can change: from a "kink," as in Fig. 3(b); or from a separate component of the dividing curve that bounds a closed disk, as in Fig. 3(c). A result of Honda [46] establishes that "kinks" can always be removed by a homotopy, so that this case reduces to that of constant k_ϕ.

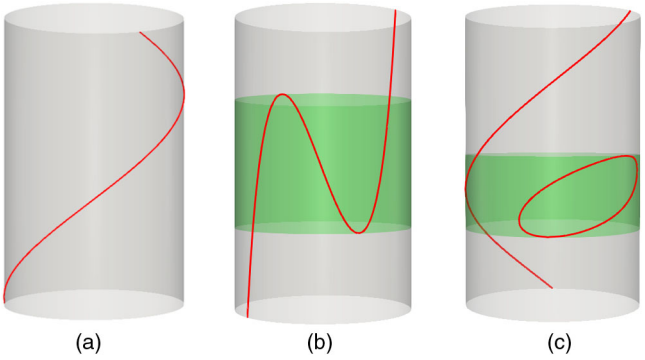

FIG. 3. Three motifs occur in the dividing curve (red) on a section of a convex torus. (a) The dividing curve turns everywhere counterclockwise and the winding k_ϕ is constant. (b) The dividing curve turns back on itself, indicating a region (green) in which $k_\phi = -1/2$, while $k_\phi = +1/2$ in the remainder of the panel. (c) There is a separate component of the dividing curve which bounds a disk on the torus, also indicating the presence of a region (green) with $k_\phi = -1/2$.

The second case, where a component of Γ bounds a disk, is more fundamental and indicates that the disclination line is overtwisted. This result is known as Giroux's criterion [20,42], which states that a component of the dividing curve bounding a disk appears if and only if there is an overtwisted disk close to the convex surface. The director on the disk bounded by Γ is a Skyrmion tube, with profile equivalent to that in Fig. 2(b), that terminates on the disclination line. A fundamental result of Eliashberg [36] states that overtwisted directors do not have any additional contact topological invariants and hence their classification is the same as that of nematics: they are classified locally by a Jänich index $\nu \in \mathbb{Z}_4$ [47,48]. Thus, overtwistedness distinguishes singular lines with an essentially varying k_ϕ from those for which k_ϕ is constant or can be made constant by the removal of kinks. In the latter case, the director is tight in a neighborhood of the singular line.

For the tight case, the dividing curve is isotopic to a rational line on the torus, or a set of rational lines all with the same slope. The examples (2), (3) cover all such possibilities, and thus any tight disclination has a neighborhood equivalent to one of these models. We will show that they have different Thurston-Bennequin invariants; it then follows from standard results of contact topology [20] that they are not homotopic. For a longitudinal Legendrian curve C on S with zero linking number with the disclination, its minimal Thurston-Bennequin number is $\overline{\mathrm{tb}} = 2q$ for the screwlike (χ) defects (2) and zero for the edgelike (τ) defects (3). For a meridional Legendrian curve, the minimal Thurston-Bennequin number is $\overline{\mathrm{tb}} = 2|1 - k|$ for both screwlike and edgelike defects. Since these invariants take

different values for different pairs of k, q (including the edge-type as $q = 0$), the different models $\mathbf{n}^{\chi}_{k,q}$ and $\mathbf{n}^{\mathrm{az}}_{k}$ represent all homotopically distinct chiral directors.

This completes the topological classification of singular lines in a cholesteric. We now discuss the consequences of this result beyond just the classification of chiral disclinations.

Our classification covers both nonorientable (half-integer k) and orientable (integer k) singular lines. For integer lines in a nematic the singularity in the director can be removed by "escape in the third dimension." This process extends to cholesterics only for negative windings and when k is positive the chiral escape is frustrated [23,48]. The removal of such a singular line either results in regions where the twist has the wrong handedness [21], or else requires the introduction of point defects. For instance, a $\mathbf{n}^{\chi}_{+1,q}$ line is replaced by a string of $2q$ point defects of alternating charge. When $q = 1$, the resulting pair of defects is a toron [49]. Longer strings of point defects arising from the removal of this type of singularity occur in cholesteric droplets and shells [14,15], where the spherical geometry naturally promotes the formation of a $\mathbf{n}^{\chi}_{+1,q}$ line, and have recently been observed in chromonic liquid crystals in a cylindrical geometry [23]. Higher charge χ lines, locally equivalent to $\mathbf{n}^{\chi}_{+2,q}$, also occur naturally in a spherical geometry [14,15]. Rather than splitting into a pair of $\mathbf{n}^{\chi}_{+1,q}$ lines, these split into a pair of $\mathbf{n}^{\tau}_{1}$ which are wrapped helically around one another, which may then be removed via escape—this structure is also predicted by our classification.

The dichotomy between overtwisted and tight disclinations has implications for the crossing of disclination lines. Classical homotopy theory arguments applied to cholesterics show that crossing two disclinations produces a λ^{+1} line tether connecting them [50]. Consequently, if we take two tight disclination lines in a cholesteric and pass one through the other, we end up with a pair of disclination lines tethered to a λ^{+1} line, which implies the disclination lines are overtwisted after the crossing event. Further analysis of the crossing and reconnection of defects using methods of contact topology would be an important extension of Ref. [50].

The director can be obtained from three-dimensional imaging techniques such as fluorescent confocal polarising microscopy (FCPM) [31,32]. Generically, each image slice will be a convex surface and those parts where the director is tangent to it form the dividing curve. This facilitates the direct analysis of experimental images to compute topological data and track layer changes using the convex surface techniques we have described. The example of Fig. 2(c) illustrates this process. To identify the class of disclination lines the fully reconstructed director field is needed to extract the data from a surface surrounding the disclination.

This work was supported by the UK EPSRC through Grant No. EP/L015374/1. J. P. is supported by a Warwick IAS Early Career Fellowship.

*joseph.pollard@durham.ac.uk
†G.P.Alexander@warwick.ac.uk

[1] N. D. Mermin, The topological theory of defects in ordered media, Rev. Mod. Phys. **51**, 591 (1979).
[2] M. V. Kurik and O. D. Lavrentovich, Defects in liquid crystals: Homotopy theory and experimental studies, Sov. Phys. Usp. **31**, 196 (1988).
[3] M. Kleman, Defects in liquid crystals, Rep. Prog. Phys. **52**, 555 (1989).
[4] G. P. Alexander, B. G. Chen, E. A. Matsumoto, and R. D. Kamien, Colloquium: Disclination loops, point defects and all that in nematic liquid crystals, Rev. Mod. Phys. **84**, 497 (2012).
[5] T. Machon and G. P. Alexander, Global defect topology in nematic liquid crystals, Proc. R. Soc. A **472**, 20160265 (2016).
[6] B. G. Chen, P. J. Ackerman, G. P. Alexander, R. D. Kamien, and I. I. Smalyukh, Generating the Hopf Fibration Experimentally in Nematic Liquid Crystals, Phys. Rev. Lett. **110**, 237801 (2013).
[7] J.-S. Wu and I. I. Smalyukh, Hopfions, heliknotons, skyrmions, torons and both Abelian and non-Abelian vortices in chiral liquid crystals, Liq. Cryst. Rev. 1 (2022).
[8] V. Poénaru, Some aspects of the theory of defects of ordered media and gauge fields related to foliations, Commun. Math. Phys. **80**, 127 (1981).
[9] B. G. Chen, G. P. Alexander, and R. D. Kamien, Symmetry breaking in smectics and surface models of their singularities, Proc. Natl. Acad. Sci. U.S.A. **106**, 15577 (2009).
[10] T. Machon, H. Aharoni, Y. Hu, and R. D. Kamien, Aspects of topology in smectic liquid crystals, Commun. Math. Phys. **372**, 525 (2019).
[11] D. C. Wright and N. D. Mermin, Crystalline liquids: The blue phases, Rev. Mod. Phys. **61**, 365 (1989).
[12] S. Čopar and S. Žumer, Nematic disclinations as twisted ribbons, Phys. Rev. E **84**, 051702 (2011).
[13] S. Čopar and S. Žumer, Nematic Braids: Topological Invariants and Rewiring of Disclinations, Phys. Rev. Lett. **106**, 177801 (2011).
[14] D. Seč, T. Porenta, M. Ravnik, and S. Žumer, Geometrical frustration of chiral ordering in cholesteric droplets, Soft Matter **8**, 11982 (2012).
[15] A. Darmon, M. Benzaquen, S. Čopar, O. Dauchot, and T. Lopez-Leon, Topological defects in cholesteric liquid crystal shells, Soft Matter **12**, 9280 (2016).
[16] A. Darmon, M. Benzaquen, D. Seč, S. Čopar, O. Dauchot, and T. Lopez-Leon, Waltzing route toward double-helix formation in cholesteric shells, Proc. Natl. Acad. Sci. U.S.A. **113**, 9469 (2016).
[17] G. Posnjak, S. Čopar, and I. Muševič, Hidden topological constellations and polyvalent charges in chiral nematic droplets, Nat. Commun. **8**, 14594 (2017).

[18] J.-S. B. Tai and I. I. Smalyukh, Three-dimensional crystals of adaptive knots, Science **365**, 1449 (2019).

[19] T. Machon, Contact topology and the structure and dynamics of cholesterics, New J. Phys. **19**, 113030 (2017).

[20] H. Geiges, *An Introduction to Contact Topology*, Cambridge Studies in Advanced Mathematics (Cambridge University Press, Cambridge, 2008), Vol. 109.

[21] J. Pollard, G. Posnjak, S. Čopar, I. Muševič, and G. P. Alexander, Point Defects, Topological Chirality, and Singularity Theory in Cholesteric Liquid-Crystal Droplets, Phys. Rev. X **9**, 021004 (2019).

[22] Y. Hu and T. Machon, Stability of highly-twisted Skyrmions from contact topology, arXiv:2102.13126.

[23] J. Eun, J. Pollard, S.-J. Kim, T. Machon, and J. Jeong, Layering transitions and metastable structures of cholesteric liquid crystals in cylindrical confinement, Proc. Natl. Acad. Sci. U.S.A. **118**, 33 (2021).

[24] Y. Han, J. Dalby, B. Carter, A. Majumdar, and T. Machon, Uniaxial versus biaxial pathways in one-dimensional cholesteric liquid crystals, Phys. Rev. Res. **4**, L032018 (2022).

[25] M. Kleman and J. Friedel, Lignes de dislocation dans les cholestériques, J. Phys. II (France) **30**, C4 (1969).

[26] G. E. Volovik and V. P. Mineev, Investigation of singularities in superfluid He_3 in liquid crystals by the homotopic topology methods, Sov. Phys. JETP **45**, 1186 (1977).

[27] Y. Bouligand, B. Derrida, V. Poenaru, Y. Pomeau, and G. Toulouse, Distortions with double topological character: The case of cholesterics, J. Phys. II (France) **39**, 863 (1978).

[28] E. Efrati and W. T. M. Irvine, Orientation Dependent Handedness and Chiral Design, Phys. Rev. X **4**, 011003 (2014).

[29] D. A. Beller, T. Machon, S. Čopar, D. M. Sussman, G. P. Alexander, R. D. Kamien, and R. A. Mosna, Geometry of the Cholesteric Phase, Phys. Rev. X **4**, 031050 (2014).

[30] T. Machon and G. P. Alexander, Umbilic Lines in Orientational Order, Phys. Rev. X **6**, 011033 (2016).

[31] I. I. Smalyukh, S. Shiyanovskii, and O. Lavrentovich, Three-dimensional imaging of orientational order by fluorescence confocal polarizing microscopy, Chem. Phys. Lett. **336**, 88 (2001).

[32] G. Posnjak, Topological formations in chiral nematic droplets, Ph.D. thesis, University of Ljubjana, 2017.

[33] K. Jänich, Topological properties of ordinary nematics in 3-space, Acta Appl. Math. **8**, 65 (1987).

[34] J. Friedel and P. G. de Gennes, Boulces de disclinations dans les cristaux liquides, C. R. Acad. Sci. Paris B **268**, 257 (1969).

[35] J. Binysh, Ž. Kos, S. Čopar, M. Ravnik, and G. P. Alexander, Three-Dimensional Active Defect Loops, Phys. Rev. Lett. **124**, 088001 (2020).

[36] Y. Eliashberg, Classification of overtwisted contact structures on 3-manifolds, Inventiones Mathematicae **98**, 623 (1989).

[37] J. Binysh and G. P. Alexander, Maxwell's theory of solid angle and the construction of knotted fields, J. Phys. A **51**, 385202 (2018).

[38] Y. Bouligand, Recherches sur les textures des états mésomorphes. 6-Dislocations coins et signification des cloisons de Grandjean-Cano dans les cholestériques, J. Phys. II (France) **35**, 959 (1974).

[39] S. Masuda, T. Nose, and U. Sato, Cross-sectional observations of the cholesteric texture in a Cano wedge cell, Liq. Cryst. **20**, 577 (1995).

[40] I. I. Smalyukh and O. D. Lavrentovich, Three-dimensional director structures of defects in Grandjean-Cano wedges of cholesteric liquid crystals studied by fluorescence confocal polarizing microscopy, Phys. Rev. E **66**, 051703 (2002).

[41] M. Wang, Y. Li, and H. Yokoyama, Artificial web of disclination lines in nematic liquid crystals, Nat. Commun. **8**, 388 (2017).

[42] E. Giroux, Convexité en topologie de contact, Commun. Math. Helv. **66**, 637 (1991).

[43] J. Pollard and G. P. Alexander, Intrinsic geometry and director reconstruction for three-dimensional liquid crystals, New J. Phys. **23**, 063006 (2021).

[44] S. Čopar and S. Žumer, Topological and geometric decomposition of nematic textures, Phys. Rev. E **85**, 031701 (2012).

[45] This formula differs slightly from that employed in the literature in contact topology [20], where it is usually assumed that contact structures are left-handed, $\mathbf{n} \cdot \nabla \times \mathbf{n} > 0$. Our definition assumes the cholesteric is right-handed—for a left-handed cholesteric, we must flip the sign of (6). Furthermore, as the contact topology literature assumes contact structures are orientable, it is customary to count only full 2π twists, leading to a factor of $1/2$ in (6).

[46] K. Honda, On the classification of tight contact structures I, Geom. Topol. **4**, 309 (2000).

[47] Note that, since every point defect has an overtwisted neighborhood [21], this also implies chiral point defects possess no homotopy invariants besides the defect charge.

[48] J. Pollard, The topology and geometry of liquid crystals, Ph.D. thesis, University of Warwick, 2020.

[49] I. I. Smalyukh, Y. Lansac, N. A. Clark, and R. P. Trivedi, Three-dimensional structure and multistable optical switching of triple-twisted particle-like excitations in anisotropic fluids, Nat. Mater. **9**, 139 (2010).

[50] V. Poenaru and G. Toulouse, The crossing of defects in ordered media and the topology of 3-manifolds, J. Phys. II (France) **38**, 887 (1977).